Original Paper Environ. Control Biol., **50** (2), 91–100, 2012

Laser-Induced Chlorophyll Fluorescence Measurement System to Assess Photosynthetic Status within Leaves

Taiken NAKASHIMA[1], Yuji YASUKOCHI[2], Shoji YAMASHITA[3], Takuya ARAKI[4] and Osamu UENO[3]

[1] *Graduate School of Bioresource and Bioenvironmental Sciences, Kyushu University, Hakozaki 6–10–1, Higashi-ku, Fukuoka 812–8581, Japan*
[2] *Yuji Kikaku Co., Ltd., Uchihashi 111–1–101, Kasuya-cho, Kasuya-gun, Fukuoka 811–2308, Japan*
[3] *Faculty of Agriculture, Kyushu University, Hakozaki 6–10–1, Higashi-ku, Fukuoka 812–8581, Japan*
[4] *Faculty of Agriculture, Ehime University, Tarumi 3–5–7, Matsuyama, Ehime 790–8566, Japan*

(Received December 26, 2011; Accepted March 19, 2012)

Chlorophyll (Chl) fluorescence measured on a leaf surface only provides the photosynthetic status of chloroplasts near the surface due to self-shading effect of Chl. Here, we report a laser-induced Chl fluorescence measurement system, which enables measurement of fluorescence induction kinetics at different tissues within a leaf as well as on both leaf surfaces, to assess photosynthetic status within leaves. The logarithmic time-scaled Chl fluorescence induction kinetics obtained from *Chenopodium album* leaves showed polyphasic transients in which four inflection points designated as O, J, I and P, were observed. Adaxial surface and palisade mesophyll showed significantly higher fluorescence intensities at O than abaxial surface and spongy mesophyll, respectively. In contrast, fluorescence intensities at J, I and P were significantly higher at abaxial surface and spongy mesophyll. Using these fluorescence intensities, the JIP test was performed. The results of JIP test indicated that adaxial surface and palisade mesophyll are characterized by lower maximum quantum yield of photosystem II (PSII) and net rate of PSII closure, but higher rate of energy transfer into electron transport chain than abaxial surface and spongy mesophyll. Considering these dorsiventral and intra-leaf variations in Chl fluorescence parameters, this study suggested the necessity of Chl fluorescence measurements on tissues as well as both surfaces to evaluate photosynthetic status of a whole leaf.

Keywords : adaxial and abaxial leaf surfaces, *Chenopodium album* L., fast induction kinetics, JIP test, palisade and spongy mesophylls

INTRODUCTION

Chlorophyll (Chl) fluorescence measurement has been used extensively as a simple and reliable technique to assess photosynthetic performance of plants nondestructively (Baker and Rosenqvist, 2004; Takayama and Nishina, 2009). However, there is an increasing number of debates concerning that Chl fluorescence obtained from a leaf surface only reflects physiological status of photosynthetic cells near the surface on which measurement is carried out (Lichtenthaler

Corresponding author : Taiken Nakashima, fax : +81–92–642–2833,
e-mail : tnak005@agr.kyushu-u.ac.jp

et al., 2005; Losciale et al., 2008; Oguchi et al., 2011). This is primarily due to self-shading effect of Chl. That is, when Chl fluorescence measurement was made on adaxial surface of leaves, excitation light is intensively absorbed by Chl at upper tissue layers and thereby Chl at deeper tissue receives limited light intensity (Schindler and Lichtenthaler, 1994). Moreover, fluorescence emitted at deeper tissues is likely to be reabsorbed by Chl that resides in upper tissues (Lichtenthaler et al., 2005). Therefore, Chl fluorescence parameters obtained in such a way depend exclusively on physiological status of upper tissues, and those of deeper tissue is largely ignored.

The dissimilarities between adaxial and abaxial sides of leaves in terms of anatomical and biochemical properties influence the photosynthetic status within a leaf. In most bifacial leaves, stomata are more abundant on abaxial than adaxial surface, and mesophyll tissues are differentiated into densely packed long palisade mesophyll cells and sparse spongy mesophyll cells surrounded by intracellular airspaces (Smith et al., 1997). These two cell types also differ in pigment composition, ultrastructure of chloroplasts and contents of photosynthetic enzymes (Terashima and Inoue, 1985). Such differences between palisade and spongy mesophyll tissues cause gradient in photosynthetic capacity inside a leaf (Evans and Vogelman, 2003). It has been also reported previously that the contribution of abaxial leaf half to whole leaf photosynthesis is significantly larger than that of adaxial leaf half in cucumber leaves (Yasutake et al., 2000).

Because of those dorsiventral heterogeneities in leaf anatomy and biochemical composition, Chl fluorescence parameters obtained from a single leaf surface would not represent the photosynthetic characteristics of a whole leaf. Therefore, it is desirable to monitor Chl fluorescence on both leaf surfaces (Lichtenthaler et al., 2005), and more ideally, at different tissue levels within leaves so as to assess photosynthetic status of a whole leaf. For this purpose, we established a laser-induced fluorescence (LIF) measurement system which enables in vivo excitation and detection of Chl fluorescence under a light microscope. Using this system, we assessed Chl fluorescence induction kinetics at different tissue layers within leaves of a C_3 dicot, *Chenopodium album* L.

MATERIALS AND METHODS

Plant materials and growth conditions

Seeds of *Chenopodium album* L. were germinated on a nursery box filled with loam soil granules and grown for 3 weeks in a greenhouse at Kyushu University (33°35′N, 130°23′E). Seedlings were then transplanted to 5 L pots containing sandy loam soil incorporated with 9.82 g of 16:16:16 synthetic N:P:K fertilizer. Plants were further grown outdoors for 4 weeks in September 2011 and uppermost fully expanded leaves from 3 plants were used for the following experiments.

LIF measurement system

LIF measurement was conducted using a system depicted in Fig. 1. A 5 mW helium-neon (He-Ne) laser (1125P, JDS Uniphase Corp., California, USA) was guided into a light microscope (YKCBM132, Yuji Kikaku Co., Ltd., Fukuoka, Japan) through an optical quartz fiber (ϕ 400 μm). The laser intensity was adjusted by combined application of neutral density (ND) and polarizing filters settled in light pass between the laser source and fiber coupling instrument. Inside the microscope, the beam was reflected by a dichroic mirror (98% reflectance at $\lambda = 580$–651 nm, 90% transmittance at $\lambda = 670$–800 nm) deployed at 45° and focused onto leaf samples under an objective lens. Chl fluorescence transmitted through the dichroic mirror was detected by a photomultiplier tube (PMT; R646, Hamamatsu Photonics K.K., Shizuoka, Japan) connected to the microscope with another optical quartz fiber (ϕ 600 μm). A high performance long-pass filter was embedded in front of the PMT to exclude the partially transmitted laser (Fig. 2A). The signal from PMT was recorded by a digital oscilloscope (DS-8812, Iwatsu Electric Co., Ltd., Tokyo, Japan) at 20 μs intervals and transferred to a personal computer for data analysis thereafter.

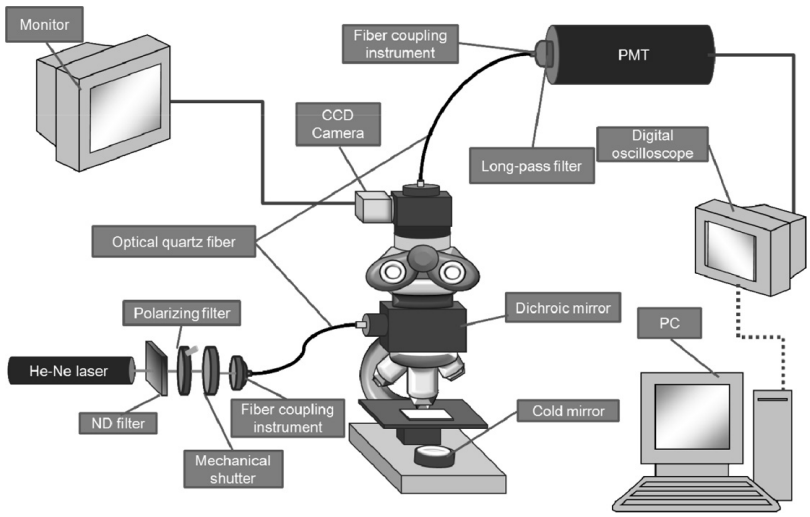

Fig. 1 Schematic diagram of Laser-induced fluorescence measurement system. He-Ne, helium-neon; ND, neutral density; CCD, charge coupled device; PC, personal computer; PMT, Photomultiplier tube.

Spectral properties of Chl florescence, laser and optical filters

The emission spectra of He-Ne laser and Chl fluorescence and transmission spectra of optical filters presented in Fig. 2 were obtained by using a spectroscope (SA-100W-HPCB/C, Lambda Vision Inc., Kanagawa, Japan). For the measurement of He-Ne laser spectrum (Fig. 2A), the laser source was directly delivered to the spectroscope with an optical quartz fiber. For the measurement of Chl fluorescence spectra (Fig. 2A), on the other hand, PMT in Fig. 1 was replaced by the spectroscope, and Chl fluorescence spectrum from adaxial surface of a *C. album* leaf was measured.

Transmission spectra of the high performance long-pass filter (Fig. 2A) and cold mirror (Fig. 2B) were measured by the spectroscope coupled with an optical quartz fiber whose end was vertically oriented towards a halogen light source (MHF-150L, Moritex Corp., Tokyo, Japan) at approximately 5 cm distance. The background halogen light spectrum (Fig. 2B) was recorded once before the measurements, and spectra of filter-transmitted light were measured by placing filters immediately above the fiber end. The transmittances (T) at different wavelengths were calculated from equation (1).

$$T(\%) = I/I_0 \times 100 \quad (1)$$

where I_0 and I denote background and transmitted light intensity at given wavelengths, respectively.

Measurements of transmittances of ND and polarizing filters

Three ND filters designated as high, medium, and low strengths were examined for He-Ne laser transmittance (Fig. 3A). The laser was guided directly into the PMT through an optical quartz fiber, and the full laser intensity without application of ND filter was measured as background. Subsequently, laser intensities with ND filter of different strength were measured, and transmittances were derived from equation 1. Similarly, transmittances of the polarizing filter at various filter angles were measured (Fig. 3B). Using those values, the photon flux density (PFD) of excitation laser was calculated as equation 2.

$$\text{PFD } (\mu\text{mol m}^{-2}\text{ s}^{-1}) = (L\ T_{ND}\ T_{PF})\ 3.186\ e^{15} / N_A / A_L \quad (2)$$

where L denotes the full laser intensity in mW under objective lens of given magnification; T_{ND} and T_{PF} represent transmittances of ND and polarizing filters, respectively; N_A and A_L represent

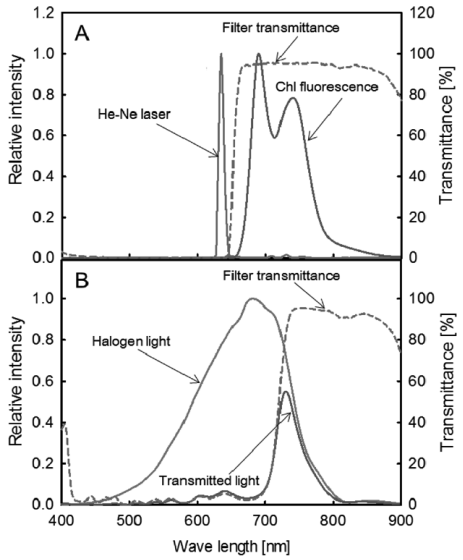

Fig. 2 Spectra of He-Ne laser and Chl fluorescence and transmission spectra of the long pass filter embedded in front of photomultiplier tube (A), and spectra of halogen light and the filter transmitted halogen light and transmission spectrum of cold mirror (B). Relative intensities of He-Ne laser, Chl fluorescence and halogen light were normalized to the peak intensities, whereas that of filter-transmitted was normalized to peak intensity of halogen light.

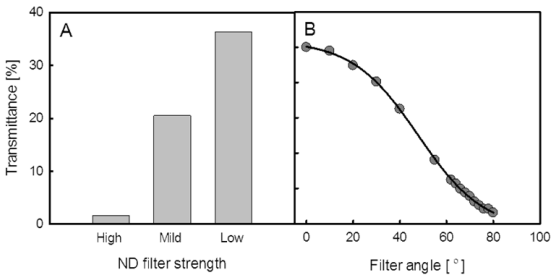

Fig. 3 Transmittances of three ND filters which differ in attenuation strength (A) and of polarizing filter at various filter angles (B).

Avogadro number and area of laser beam cross-section, respectively. Under ×5 and ×40 objective lenses, measured L were 0.85 and 0.33 mW, respectively. In addition, transmittance of coverslip (98.1%) was also taken into account for PFD calculation under ×40 objective lens.

LIF measurement at leaf surface and tissue levels

LIF measurement was conducted at two resolutions; at leaf surface and tissue levels. In the former, Chl fluorescence was measured at both adaxial and abaxial leaf surfaces. Upon the measurement, two leaf discs were excised from adjacent areas of an overnight dark-adapted leaf and mounted with a drop of distilled water on a glass slide. Each leaf disc facing either adaxial or abaxial side upward was focused under ×5 objective lens. To avoid excitation of leaf samples during focus adjustment, the halogen source under sample stage was filtered by a cold-mirror which blocks wavebands below 700 nm as shown in Fig. 2B. The induction kinetics of Chl fluorescence was recorded for 2 s at five different spots of approximately 330 μm in diameter. The same procedure was repeated for the leaf disc facing abaxial surface upward.

For tissue level measurements, a leaf disc was sampled from adjacent area where two leaf discs were sampled previously, and hand-sectioned to yield a cross-section of approximately 50 μm thickness. The cross-section was mounted on buffer solution containing 0.65 M sorbitol, 1 mM $CaCl_2$, 0.5 mM $MgCl_2$, 10 mM HEPES (N-2-hydroxyethylpiperazine-N′-2-ethanesulfonic acid; pH 7.0) (Riazunnisa et al., 2007) and focused under the ×40 objective lens. Measurements were taken from 4 different tissue layers, namely, upper palisade (UPM), lower palisade (LPM), upper spongy (USM) and lower spongy mesophylls (LSM) as indicated in Fig. 4. For each layer, the measurements were repeated at five different spots of approximately 40 μm in diameter.

All the data obtained from leaf surfaces and different tissue layers were presented as means of 15 individual measurements from 3 plants.

Analysis of Chl induction kinetics by the JIP test

Chl fluorescence induction kinetics with logarithmic time scale exhibits a polyphasic transient with inflection points at 0.05, 0.3, 2 and 30 ms after the onset of excitation (Govindjee, 1995). By defining the fluorescence intensities at these inflection points as F_o, $F_{300\,\mu s}$, F_J and F_I, respectively, and the maximum fluorescence intensity as F_P, the JIP test originally developed by Strasser and Strasser (1995) was performed to parameterize photosynthetic status of leaf tissues. The parameters of JIP test described below were calculated according to van Heerden et al. (2003).

The maximum quantum yield of photosystem II (PSII) (ϕ_{PO}), which reflects the probability that an absorbed photon will be trapped by the PSII reaction center (RC), was derived from equation 3.

$$\phi_{PO} = 1 - F_o / F_P \tag{3}$$

The approximate value of the initial slope of induction curve (M_o), a parameter interpreted as net rate of PSII closure, was calculated as equation (4).

$$M_o = 4(F_{300\,\mu s} - F_o) / (F_P - F_o) \tag{4}$$

The electron transport probability (ψ_o), representing the efficiency of trapped excitation energy to be transferred to electron transport chain (ETC) beyond primary quinone acceptor (Q_A), was derived from equation (5).

$$\psi_o = 1 - V_J = 1 - (F_J - F_o) / (F_P - F_o) \tag{5}$$

The performance index (*PI*), a multi-parametric expression of these three independent steps contributing to photosynthesis, was calculated from equation 6.

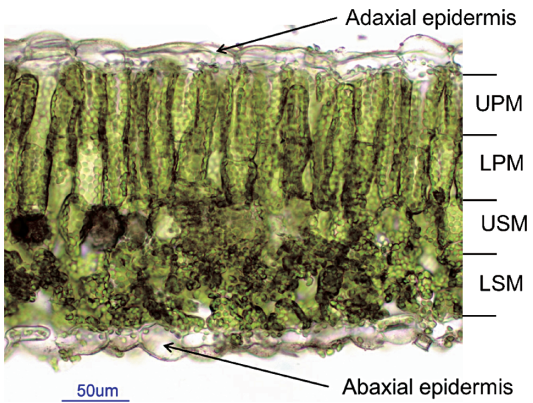

Fig. 4 Hand cut section of *Chenopodium album* leaf. Bar = 50 μm. UPM, upper palisade mesophyll; LPM, lower palisade mesophyll; USM, upper spongy mesophyll; LSM, lower spongy mesophyll.

$$PI = RC/ABS\ [(\phi_{Po} / (1-\phi_{Po})][\psi_o / (1-\psi_o)] \quad (6)$$

where *RC*/*ABS* represents reaction centers per absorbed energy flux.

Determination of optimal excitation laser intensity

To determine optimal excitation laser intensity to obtain a polyphasic O-J-I-P transient of Chl fluorescence, LIF measurements were made under different excitation laser intensity. The ND filters of medium and high strength were used for measurements at leaf surface and tissue levels, respectively, and a precise adjustment of laser intensity was made by rotating the polarizing filter. The measurements were conducted on adaxial surface and at UPM.

Statistical analysis

Statistical analysis was made by using SigmaPlot 12 (Systat Software Inc., Illinois, USA). Student *t*-test was performed for comparison between adaxial and abaxial data with means of 15 individual measurements. For comparisons among data from different tissues, Tukey's range test ($P < 0.05$) was performed on means of 15 individual measurements.

RESULTS AND DISCUSSION

Optical performance of filters and lenses

Emission spectrum of Chl fluorescence showed double peaks at 690 and 740 nm, the former of which was relatively close to the peak of He-Ne laser (633 nm) (Fig. 2A). Therefore, a high performance long-pass filter was placed in front of PMT to ensure exclusion of partially reflected He-Ne laser from Chl fluorescence signal. The long-pass filter showed negligibly low transmittance at 633 nm while showing remarkably high transmittance above 660 nm (>95%), confirming successful separation of He-Ne laser and Chl fluorescence at around 640 nm with small loss of fluorescence intensity.

Another optical filter, a cold mirror, was applied onto a halogen light source beneath the sample stage to avoid excitation of leaf samples during focus adjustment (Fig. 1). The measured halogen light spectrum was rich in red wavebands with a peak at 680 nm, which is preferentially absorbed by Chl (Fig. 2B). The application of the filter, which selectively transmits far-red wavebands efficiently but not red wavebands, generated light spectrum peaked at 730 nm (Fig. 2B). Since far-red light is absorbed less intensively by Chl, the filter application allowed us to perform repetitive focus adjustment without affecting the dark-adapted state of leaf samples.

The transmittances of three ND filters and of polarizing filter at various filter angles were obtained for PFD calculation of excitation laser (Fig. 3). ND filters of low, medium and high attenuation strength showed transmittances of 36.9, 21.4 and 2.6%, respectively (Fig. 3A). The medium and high ND filters were selected for a coarse adjustment of laser intensity to generate roughly equal PFD under ×5 and ×40 objective lenses, respectively. Transmittance of the polarizing filter was the highest at filter angle of 0° and decreased consecutively with increasing filter angle (Fig. 3B). Therefore, more precise adjustment of laser intensity was done by rotating the polarizing filter, and the optimal laser intensities for the measurements were determined in the following section.

Effects of laser intensity on Chl fluorescence induction kinetics

Fluorescence intensity and overall shape of Chl fluorescence induction curve was largely influenced by excitation laser intensity (Fig. 5). When the measurements were made on adaxial leaf surface at lower laser intensity (the polarizing filter angle of 60°), the transient curve showed flattened O-J rise with marked I-P rise (Fig. 5A) as reported previously (Hsu and Leu, 2003; Shansker et al., 2006). An increase in laser intensity by adjusting the filter angle to 20° drastically elevated overall fluorescence intensity with O-J-I-P transient (Fig. 5A). Further increase in laser intensity (the filter angle 0°) slightly altered the fluorescence intensity and shape of the curve (Fig. 5A).

Similarly, Chl fluorescence kinetics measured on UPM showed flattened O-J-I rise at lower

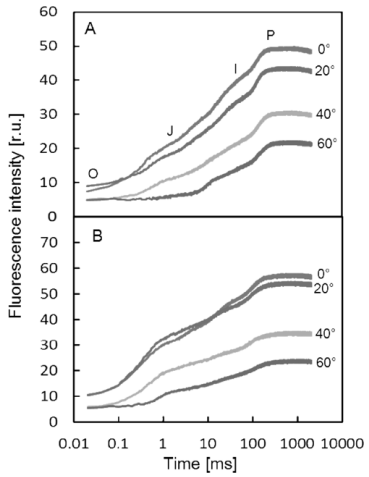

Fig. 5 Logarithmic time-scaled Chl fluorescence induction kinetics at different polarized filter angles. The measurements were carried out on adaxial leaf surface (A) and upper palisade mesophyll (B). O, J and I indicate inflection points at 0.05, 2 and 30 ms, respectively and P indicates point where fluorescence intensity reached the maximum. The values are means of 15 individual measurements taken from 3 plants.

laser intensities (the filter angles of 60° and 40°), and difference in fluorescence intensity was not almost observed between the filter angles of 20° and 0° (Fig. 5B). Therefore, it became clear that the filter angle of 20° generated optimum laser intensity for both leaf surface and tissue level measurements.

The calculated PFD of excitation laser delivered at surfaces of leaf discs and cross-sections were approximately 10,350 and 10,450 μmol m^{-2} s^{-1}, respectively. Actinic light intensity used in previous studies ranged from 10 to 15,000 μmol m^{-2} s^{-1} (Shansker et al., 2006; Takayama et al., 2010), among which 3,000 μmol m^{-2} s^{-1} was more frequently used. However, Shansker et al. (2006) reported that increases in PFD from 1,800 to 15,000 μmol m^{-2} s^{-1} had no apparent effect on quality of fluorescence kinetics. Since higher fluorescence intensity reduces noise to fluorescence signal ratio, the high intensity of excitation laser is preferable for attaining a certain level of accuracy in this system.

Chl fluorescence induction kinetics on adaxial and abaxial surfaces

The overall shape as well as fluorescence intensities of induction kinetics differed remarkably between adaxial and abaxial leaf surfaces (Fig. 6A). The curve obtained from abaxial surface showed pronounced polyphasic transient with significantly higher F_J, F_I and F_P values than that of adaxial surface (Fig. 6A and Table 1). In contrast, F_o was significantly higher at adaxial than at abaxial surface. The higher fluorescence intensities and steeper initial slopes of induction kinetics at abaxial surface have been reported previously for various plant species (Schreiber et al., 1977).

The higher F_P and lower F_o at abaxial surface resulted in higher ϕ_{PO} than adaxial surface (Table 1). Moreover, initial slope was also steeper at abaxial surface than at adaxial surface, as indicated by significantly higher M_o (Table 1). On the other hand, ψ_o, a parameter reflecting electron transport capacity beyond Q_A^-, was significantly higher at adaxial surface. The overall performance of photochemical reactions expressed as *PI* was therefore higher at the adaxial surface than the abaxial surface (Table 1).

Chl fluorescence induction kinetics at different tissue levels

The induction kinetics of Chl fluorescence measured on different tissue levels varied significantly in F_o, F_J, F_I and F_P (Fig. 6B and Table 1). The F_J, F_I and F_P were the lowest at UPM and

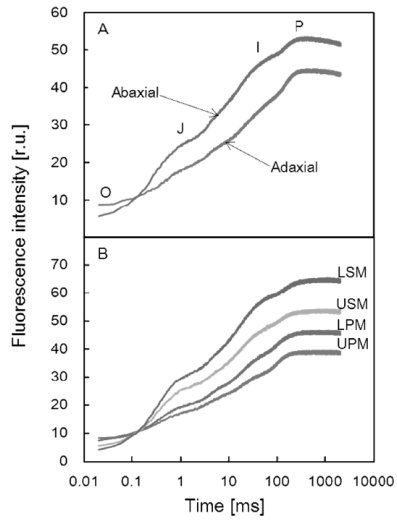

Fig. 6 Logarithmic time-scaled Chl fluorescence induction kinetics measured at adaxial and abaxial leaf surfaces (A), and at different tissue levels (B). UPM, upper palisade mesophyll; LPM, lower palisade mesophyll; USM, upper spongy mesophhyll; LSM, lower spongy mesophyll. O, J and I indicate inflection points at 0.05, 2 and 30 ms, respectively and P indicates point where fluorescence intensity reached the maximum. The values are means of 15 individual measurements taken from 3 plants.

increased in the order of LPM＜USM＜LSM, whereas F_o increased in the reverse order (Table 1). In addition, UPM and LPM showed relatively flat O-J-I rise as compared to USM and LSM (Fig. 6B). The JIP test parameters also showed tissue-dependent variations, in which ϕ_{Po} and M_o were significantly higher for spongy mesophyll than for palisade mesophyll. In contrast, palisade mesophyll exhibited significantly higher ψ_o than spongy mesophyll. Furthermore, ϕ_{Po} and M_o showed increasing trends as tissue depth from adaxial leaf surface increased. These results were consistent with those obtained from leaf surfaces, indicating that induction kinetics measured at adaxial and abaxial leaf surfaces only reflects photosynthetic status of palisade and spongy mesophyll, respectively, but not that of a whole leaf. These results suggest the necessity of Chl fluorescence measurements on tissues as well as both surfaces to evaluate photosynthetic status of a whole leaf.

Future prospects

The LIF system developed in this study revealed dorsiventral and intra-leaf variations in Chl fluorescence induction kinetics, which has been often ignored in previous studies. Although our approach devoted a large advantage of Chl fluorescence measurement for the simplicity and non-destructiveness, further advances in this technique may provide detailed insight into differential responses of photosynthetic cells to abiotic stresses such as high light, water-deficit and extreme temperatures. Furthermore, cell-type specific measurement of Chl fluorescence may help differentially evaluating physiological responses of mesophyll and bundle sheath cells in leaves of C_4 plants to various environmental factors.

To further develop this system as a more reliable tool for cellular assessment of Chl fluorescence, the reproducibility of leaf cross-section with a constant thickness, accuracy of focus adjustment, and measurement resolution remain to be improved.

This study was supported by a grant from the Japanese Society for the Promotion of Science Research Fellowship for Young Scientists to T.N. (No. 10J01856).

Table 1 Fluorescence intensities at different inflection points of O-J-I-P transient and calculated JIP test parameters.

	Fluorescence intensity [r.u.]					JIP test parameters			
	F_o	F_J	F_I	F_P	$F_{300\,\mu s}$	ϕ_{PO}	M_o	ψ_o	PI
Adaxial	8.87±0.64***	19.8±0.95***	31.9±2.4***	46.2±2.11***	13.1±0.47***	0.81±0.02***	0.45±0.08***	0.71±0.02***	5.44±0.59***
Abaxial	6.67±0.49	26.6±1.01	44.3±1.88	54.5±1.88	17.3±0.46	0.88±0.01	0.89±0.03	0.58±0.01	4.16±0.35
UPM	8.53±1.36^a	18.6±4.39^c	29.5±6.97^d	41.3±7.77^d	13.1±1.88^c	0.78±0.07^c	0.50±0.24^b	0.72±0.1^a	4.86±1.33^b
LPM	8.33±1.29^a	20.9±3.12^c	35.3±5.54^c	48.3±5.91^c	14.0±1.4^c	0.82±0.04^b	0.55±0.16^b	0.69±0.06^a	5.33±1.4^b
USM	6.47±0.92^b	27.4±4.16^b	43.9±5.08^b	55.9±6.72^b	16.6±1.65^b	0.88±0.02^a	0.82±0.18^a	0.57±0.09^b	5.02±1.58^b
LSM	5.47±0.74^b	32.2±2.56^a	53.7±4.44^a	67.5±6.06^a	18.6±1.1^a	0.92±0.02^a	0.85±0.06^a	0.57±0.04^b	7.22±1.7^a

*** represents significant difference between adaxial and abaxial data by Student t-test ($P<0.001$). Different superscript letters represent significant differences among various tissue levels by Tukey's range test ($P<0.05$). Values are means±SD ($n=15$).

REFERENCES

Baker, N. R., Rosenqvist, E. 2004. Applications of chlorophyll fluorescence can improve crop production strategies: an examination of future possibility. J. Exp. Bot. **55**: 1607–1621.

Evans, J. R., Vogelman, T. C. 2003. Profiles of ^{14}C fixation through spinach leaves in relation to light absorption and photosynthetic capacity. Plant Cell Environ. **26**: 547–560.

Govindjee. 1995. Sixty-three years since Kautsky: Chlorophyll a fluorescence. Aust. J. Plant Physiol. **22**: 131–160.

Hsu, B.-D., Leu, K.-L. 2003. A possible origin of the middle phase of polyphasic chlorophyll fluorescence transient. Funct. Plant Biol. **30**: 571–576.

Lichtenthaler, H. K., Buschmann, C., Knapp, M. 2005. How to correctly determine the different chlorophyll fluorescence parameters and the chlorophyll fluorescence decrease ratio RFD of leaves with PAM fluorometer. Photosynthetica **41**: 379–393.

Losciale, P., Oguchi, R., Hendrickson, L., Hope, A. B., Corelli-Grappadelli, L., Chow, W. S. 2008. A rapid, whole-tissue determination of the functional fraction of PSII after photoinhibition of leaves based on flash-induced P700 redox kinetics. Physiol. Plant. **132**: 23–32.

Oguchi, R., Douwstra, P., Fujita, T., Chow, W. S., Terashima, I. 2011. Intra-leaf gradients of photoinhibition induced by different color light: implications for the dual mechanisms of photoinhibition and for the application of conventional chlorophyll fluorometers. New Phytol. **191**: 146–159.

Riazunnisa, K., Padmavathi, L., Scheibe, R., Raghavendra, A. S. 2007. Preparation of Arabidopsis mesophyll protoplasts with high rates of photosynthesis. Physiol. Plant. **129**: 679–686.

Schansker, G., Tóth, S. Z., Strasser, R. J. 2006. Dark recovery of the Chl a fluorescence transient (OJIP) after light adaptation: The qT-component of non-photochemical quenching is related to an activated photosystem I acceptor side. Biochim. Biophys. Acta **1757**: 787–797.

Schindler, C., Lichtenthaler, H. K. 1994. Photosynthetic CO_2 assimilation, chlorophyll fluorescence and zeaxanthin accumulation in field grown maple tree in the course of a sunny and a cloudy day. J. Plant Physiol. **148**: 399–412.

Schreiber, U., Fink, R., Vidaver, W. 1977. Fluorescence induction in whole leaves: Differentiation between the two leaf sides and adaptation to different light regimes. Planta **133**: 121–129.

Smith, W. K., Vogelman, T. C., Delucia, E. H., Bell, D. T., Shepherd, K. A. 1997. Leaf form and photosynthesis: Do leaf structure and orientation interact to regulate internal light and carbon dioxide? BioScience **47**: 785–793.

Strasser, B. J., Strasser, R. J. 1995. Measuring fast fluorescence transients to address environmental questions: The JIP-test. In "Photosynthesis: from Light to Biosphere" (ed. by Mathis, P.), Kluwer Academic Publisher, Dordrecht, p 977–980.

Takayama, K., Nishina, H. 2009. Chlorophyll fluorescence imaging of the chlorophyll fluorescence induction phenomenon for plant health monitoring. Environ. Control Biol. **47**: 101–109.

Takayama, K., Sakai, Y., Oizumi, T., Nishina, H. 2010. Assessment of photosynthetic dysfunction in a whole tomato plant with chlorophyll fluorescence induction imaging. Environ. Control Biol. **48**: 151–159.

Terashima, I., Inoue, Y. 1985. Palisade tissue chloroplasts and spongy tissue chloroplasts in spinach: Biochemical and ultrastructural differences. Plant Cell Physiol. **26**: 63–75.

van Heerden, P. D. R., Tsimilli-Michael, M., Krüger, G. H. J., Strasser, R. J. 2003. Dark chilling effects on soybean genotypes during vegetative development: parallel studies of CO_2 assimilation, chlorophyll a fluorescence kinetics O-J-I-P and nitrogen fixation. Physiol. Plant. **117**: 476–491.

Yasutake, D., Kitano, M., Hamakoga, M., Araki, T., Nagasuga, K., Suzuki, Y. 2000. An improved cuvette for individual evaluations of gas exchange parameters on adaxial and abaxial leaf surfaces under different air currents. Biotronics **29**: 33–42.